Ocean Dynamics (2006) 56: 26–35
DOI 10.1007/s10236-005-0041-2

Lidia Gaslikova · Ralf Weisse

Estimating near-shore wave statistics from regional hindcasts using downscaling techniques

Received: 28 February 2005 / Accepted: 30 August 2005 / Published online: 11 March 2006

Abstract Several downscaling techniques, comprising fully dynamical and statistical–dynamical methods applied to near-shore local wave climate, are tested and assessed in terms of wave statistics with respect to the added value that can be achieved compared to larger scale data. The techniques are applied for the example of Helgoland, a small island in the German Bight. It was found that an improved representation could generally be obtained from all downscaling techniques by comparing the near-shore wave climate. Based on a balance between the required computer resources and the improvements achieved, it is suggested, to this end, that a dynamical–statistical approach based on high-resolution coastal wave modeling and linear regression provides the optimal choice.

Keywords Shallow water · Wave climate · Coastal protection · Statistical downscaling

Introduction

Many applications in coastal engineering require knowledge about extreme wave statistics at or near the coastal facilities. The data for such statistics are often limited or sometimes even nonexistent. Measurements from a nearby location are frequently used instead. In combination with more or less sophisticated methods to transfer the information to the place of interest, measurements are used to derive the relevant statistics (e.g., Coastal Engineering Manual, Eurowaves project, JERICHO project). When such measurements are not available or lack homogeneity that prevents the estimation of reliable statistics, multidecadal wave hindcasts may be an alternative. In recent years, multidecadal simulations of ocean waves have become more and more common (e.g., WASA Group 1998; Günther et al. 1998; Cox and Swail 2001; Weisse et al. 2002; Caires et al. 2002; Sterl et al. 1998; Kushnir 1997). Most of these studies have been motivated by concerns about possible ongoing long-term changes in the wave climate (especially in the extreme sea states) and their consequences for coastal protection and the safety of humans living at the coast. While large-scale changes may be reasonably estimated from these simulations, their value for the design and safety assessment of coastal protection structures may be limited due to their relatively coarse spatial and temporal resolutions. Another reason for this is that shallow water effects are usually not accounted for in most of these simulations. In addition, because of computational constraints their spatial resolution remains limited and may be too coarse to be used directly for coastal design purposes. For the latter, additional techniques are required to transfer the wave information from such a hindcast to the site of the construction. Several different methods (hereafter referred to as downscaling techniques) exist for that purpose. First principles of shallow water wave processes (e.g., Coastal Engineering Manual) are frequently applied. A shallow water high-resolution wave model can be used alternatively in downscaling large-scale wave data in cases where such data are available as boundary conditions. Such simulations would be performed optimally for multidecadal periods. However, due to rather high computational costs or restricted availability of adequate boundary conditions, simulations are usually limited to few cases with different meteorological and wave conditions, for instance a few selected severe storm situations (e.g., Vierfuss 2002). While such hindcasts for selected cases may provide some additional insight, their usability for the estimation of extreme wave statistics remains limited.

The objective of this study is twofold. First, we investigate to what extent extreme wave statistics obtained from an existing multidecadal wave hindcast reproduce the small-scale near-shore features. Next, we apply different downscaling techniques and assess the additional value in

Responsible Editor: Roger Proctor

L. Gaslikova (✉) · R. Weisse
Institute for Coastal Research, GKSS Research Centre,
P.O. Box, 21502 Geesthacht, Germany
e-mail: lidia.gaslikova@gkss.de

the representation of extreme wave statistics with respect to additional computing costs required. The paper is structured as follows. In Section 2 the multidecadal wave hindcast that has been used as a reference run is described. Next, the shallow water wave model that has been used to downscale the large-scale wave hindcast, its set-up, and the experiment are described. Validation of this experiment is provided in the last part of Section 2. In Section 3, we first investigate the extent to which observed near-coastal extreme wave statistics are reproduced in the existing large-scale multidecadal wave hindcast. We also elaborate on differences in the representation of these statistics, when derived directly from the reference hindcast and the downscaled shallow water wave model experiment. Different downscaling techniques, based on the two simulations, are tested and assessed (Section 4) with respect to the improvement that could be achieved in the representation of extreme wave statistics when compared to those obtained from the coarse-grid reference run. In Section 5, our results are summarized and discussed.

Model and experiments

The large-scale multidecadal wave hindcast

We use as the reference large-scale wave data the multidecadal wave hindcast 1958–2002 for the Southern North Sea provided by Weisse et al. (2003). This simulation has been produced within the Hindcast of Dynamic Processes of the Ocean and Coastal Areas of Europe (HIPOCAS) project (Soares et al. 2002). The data set was chosen because, to our knowledge, it represents the longest homogeneous wave hindcast available at the presently unsurpassed spatial resolution of about 5.5 km and also takes into account shallow water effects. Here, the wave model WAM (WAMDI Group 1988) has been used to produce the hindcast. Two runs with different spatial resolutions were produced. A coarse run with an approximate resolution of 50×50-km covered part of the North Atlantic and the North Sea and is referred further as HCG run. A finer run with a resolution of 5×5 km covered the North Sea south from 56°N (referred as HFG run) and used the HCG data as boundary conditions. In the two simulations, wave integrated parameters (such as significant wave height, peak period, peak direction, etc.) were stored hourly and wave spectra were stored every 3 h. The two runs were driven by hourly wind fields at 50 km resolution obtained from an atmospheric hindcast performed with the REMO model (Feser et al. 2001). For the HFG run, water level variations were taken into account. Hourly water level and current components on an irregular grid (about 200 m for the German Bight) were obtained within the hindcast provided by BAW (Coastal Division of the Federal Waterways Engineering and Research Institute) using the storm–surge model TELEMAC-2D (A. Pluess, 2003, personal communication).

The shallow water wave model and experiment

For the dynamical downscaling of the reference data, the K-model (Schneggenburger et al. 1997) was adopted. The K-model represents a third generation shallow water wave model that captures features of the large-scale forcing and adds to them the small-scale effects not resolved by the driving large-scale data. It is a discrete spectral wave model solving the wave action balance equation in the wave number domain. A modified Philips linear function (Cavaleri and Rizzoli 1981) and a modified Snyder exponential function (WAMDI Group 1988) parameterize energy input by the wind. Nonlinear wave–wave interactions have been neglected following the reason of Schneggenburger (1998) who argued that in shallow water the assumptions of homogeneity for the application of this theory are violated. Instead, a nonlinear dissipation source function (Günther and Rosenthal 1995; Schneggenburger et al. 1997) accounting for the dissipation by wave turbulence is used. Bottom dissipation is taken into account according to Hasselmann et al. (1973) and wave breaking is simulated by nonlinear energy dissipation depending on water depth (Hasselmann 1974). In addition, refractions caused by currents and depth are also included. The tunable parameters were set up according to Schneggenburger (1998) set for the limited fetch growth. For a detailed description of the K-model, we refer to Schneggenburger (1998). A comparison of the model performance relative to other shallow water wave models is presented in Moghimi et al. (2005).

The model was set up for the vicinity of Helgoland, an island located in the German Bight (Fig. 1). The model domain comprises an area of about 15×15 km at a spatial resolution of 100×100 m. The bathymetry was obtained from the BAW (N. Winkel, personal communication) with a resolution of about 50 m on an unstructured grid and was interpolated to the K-model resolution. A propagation time step of 4 s was adopted. Forcing sources comprise hourly near-surface wind fields, water level, and current fields obtained from the HIPOCAS hindcasts and have been interpolated to K-model grid. As boundary conditions, 3-hourly wave spectra from HFG reference run were used. The K-model was integrated for the 12-year period 1990–2001. The results of this simulation have been stored hourly in the form of integrated wave parameters such as significant wave height, peak period, peak wave direction etc. at all grid points and as two-dimensional wave spectra at selected model grid points (see Fig. 1). In this set-up, the K-model simulation can be considered as a dynamical downscaling of the HIPOCAS wave hindcast. In the following, we will refer to this simulation as the K-model hindcast (KMH).

Validation of K-model results

In this section, we elaborate on the quality of the K-model simulation and the extent to which observed conditions are

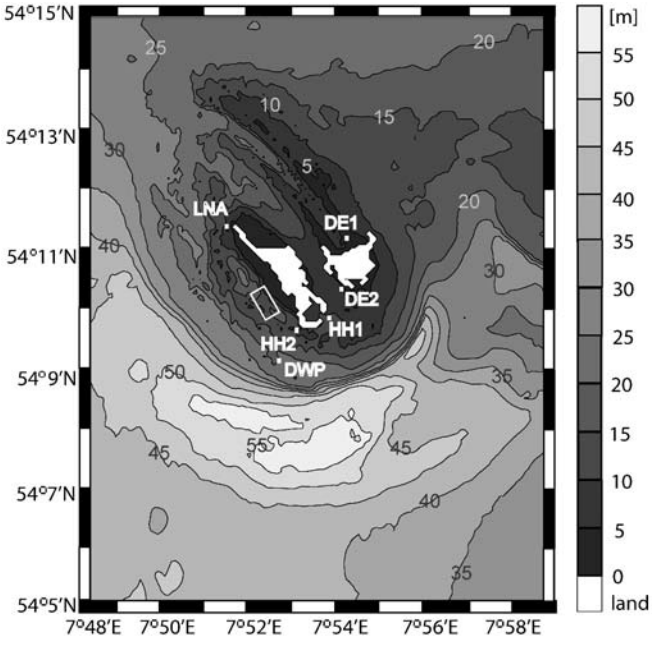

Fig. 1 K-model domain and bathymetry in meters. The location of a deepwater buoy used for validation is indicated by DWP. The *rectangle* indicates the area for which radar measurements taken from a telecommunications tower at the main island are representative. *LNA*, *HH1*, *HH2*, *DE1*, and *DE2* represent model points near coastal facilities and are used for assessing model performance

reproduced. Unfortunately, only limited data are available for the comparison. No long-term measurements exist close to coastal facilities. A wave rider buoy is located in deep water (here about 20 m) approximately 1 km southwest of the island and measures significant wave height, peak period, and peak direction. Data from this buoy for the period March 1998 to October 2001 were available. In addition, data from a WaMoS II (Wave and Surface Current Monitoring System) radar (Hessner et al. 2001), permanently mounted on a telecommunications tower on the main island since March 1998, were available for some periods within the years 1998–2001. The location of the deepwater buoy and the area covered by the radar are shown in Fig. 1. As an example, Fig. 2 shows modeled and observed significant wave height, peak period, and peak direction for October 1998. In general, a good agreement between the KMH and the observations can be inferred. For some high wave situations, significant wave heights appear to be overestimated by the model. Peak periods are slightly overestimated by the simulated data for very high waves. Wave directions are hindcast quite reasonably.

Figure 3a shows a comparison of modeled and observed significant wave height distribution for the period 1998–2001. For the lower 90% of the distribution, a rather good agreement between model and observations can be inferred. In the range between 1.0 and 1.5 m, the K-model slightly underestimates the buoy data. For the highest 10%

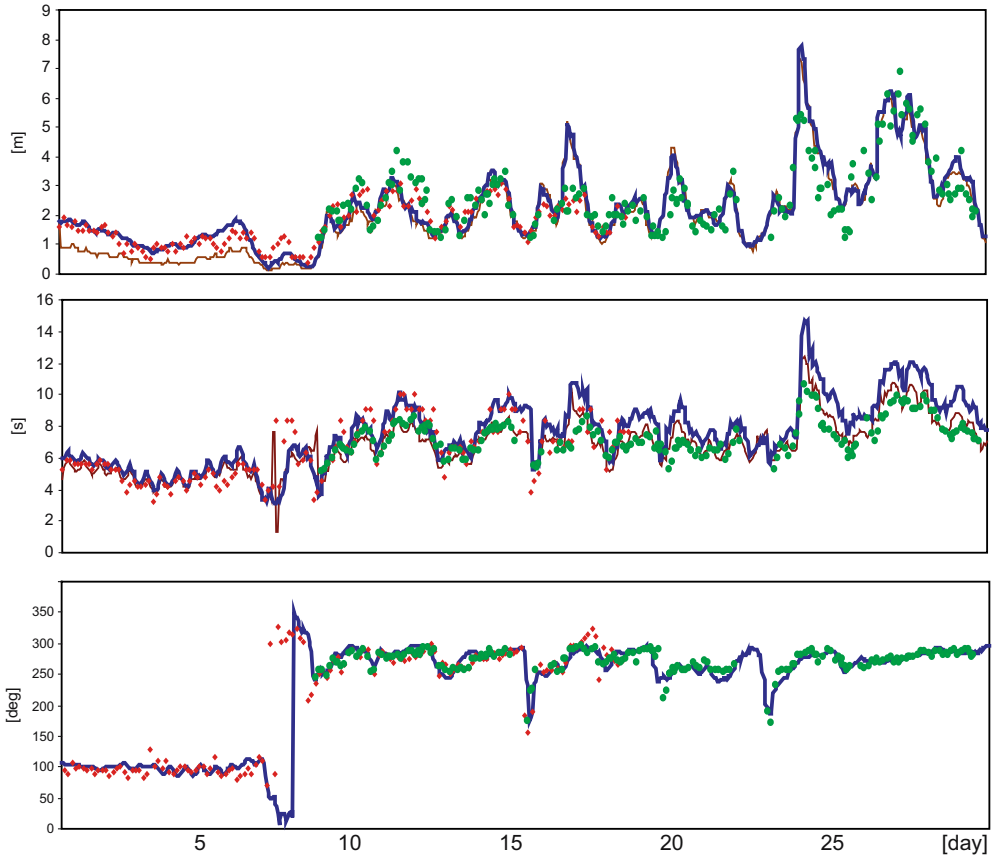

Fig. 2 Hindcast (KMH) and observed wave parameters at DWP and the central point from the area covered by radar measurements for October 1998. From *top to bottom*: significant wave height in meters, peak period in seconds and peak direction (coming from) in degrees. Buoy measurements are shown as *red crosses*, radar measurements are shown as *green circles*. The K-model hindcast at the buoy (DWP) location is given by a *blue line*; hindcast at the central point of radar rectangular is given by a *thin brown line*

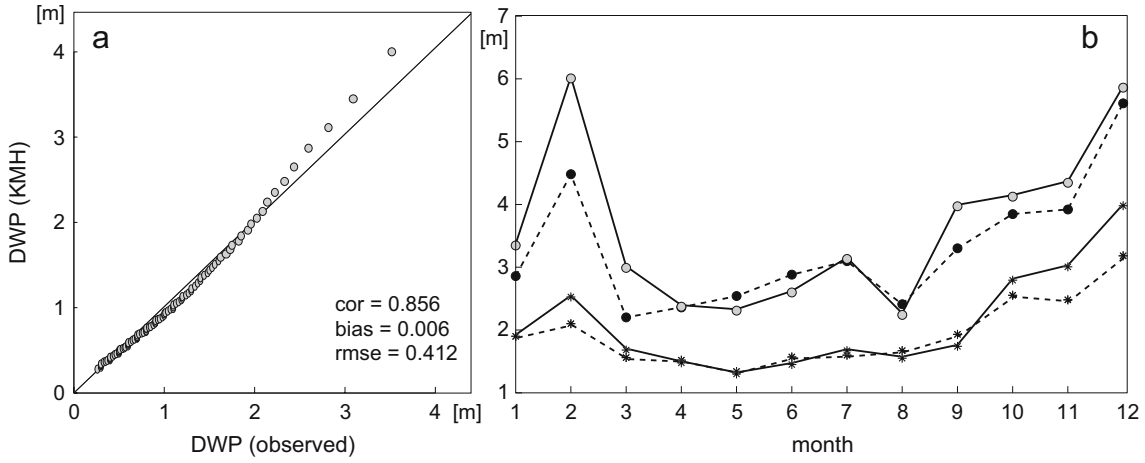

Fig. 3 **a** Quantile–quantile plot 1998–2001 of observed by buoy and hindcast significant wave height at DWP. Shown are the 5–99 percentiles. **b** Comparison of observed (*dashed*) and hindcast (*solid*) monthly 90-percentiles (*stars*) and 99-percentiles (*circles*) of significant wave height at DWP. In all cases, quantiles have been compared only for dates for which observational data have been available

of the waves, an overestimation by the K-model of up to 80 cm can be inferred, indicating that the highest waves occur too often or are too severe in the KMH simulation. A similar comparison between the HFG hindcast and the buoy data was made (not shown) to investigate the possible reasons for such a discrepancy. The overestimation of observed high waves was found to be in the same order of magnitude for the HFG run as for the K-model. This bias in upper percentiles of boundary conditions (HFG) corresponds with the results of HFG comparison with satellite data for German Bight (M. Zahn 2004, personal communication) and can be explained by deficiencies of model spatial resolution or by the uncertainties in driving force and model physics of HFG run. For the first type of errors, the K-model is supposed to improve the wave data with respect to HFG, taking into account processes on finer scales. However, this cannot be the case for the buoy position because of the relatively deep water at the location (20 m) and therefore diminished importance of the wave processes like refraction or dissipation. For the second type of the errors, the bias is expected to remain as soon as the objectively higher energy would be transferred by the K-model to the inner model locations. It can be concluded that the overestimation of the most severe wave events is partially a result of too high waves provided at the K-model boundaries.

Figure 3b shows a more detailed comparison of observed and hindcast averaged monthly 90- and 99-percentiles. For the 90-percentile, a reasonable agreement can be inferred. An exception is found in the months of November, December, and February for which the model tends to show higher extremes. A similar condition holds for the 99-percentile that represents the most extreme events. For the 99-percentile, KMH values are somewhat higher also for September and October. Possible reasons include systematic effects in the driving boundary conditions, uncertainties in bathymetry and wind data, and measurement errors. Longer observational data are required to assess fully whether the described differences between observed and hindcast frequency distribution appear to be systematic.

Despite the limited amount of available observations, we were still able to test whether systematic differences between the observations and the K-model do occur for periods for which both buoy and radar measurements have been available. Although the locations of the measurements are slightly different, the radar was calibrated to the buoy observations, which gives the opportunity to compare these two data sets and to allow them both to be compared with the results from the same location of the model domain, namely DWP. Figure 4 shows scatter plots between significant wave heights obtained from the KMH experiment at DWP, radar, and buoy data. Although a considerable scatter can be inferred between buoy and KMH (green) especially for the waves higher than 2 m, and for the pair radar KMH in the interval 1–2 m and also for

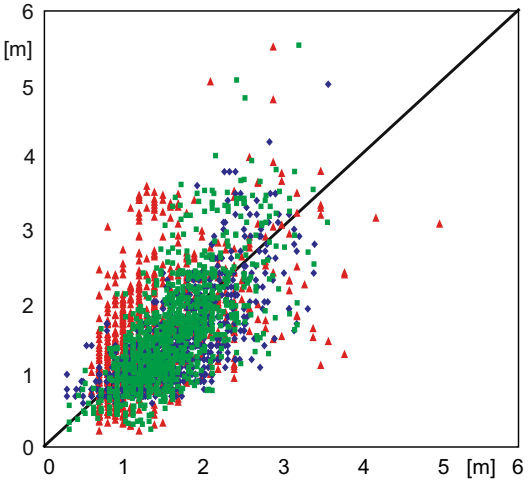

Fig. 4 Scatter plot between modeled and observed significant wave height in meters at DWP. *Green*: buoy measurements (*x-axis*) vs. KMH (*y-axis*); *Red*: radar (*x-axis*) vs. KMH (*y-axis*); Blue: buoy (*x-axis*) vs. radar (*y-axis*)

the highest waves, similar scatter is obtained also for the pair buoy–radar. Both K-model and radar have a tendency to overestimate the highest waves with respect to the buoy but there is no systematic bias between KMH and radar extremes. From Fig. 4, it can be further concluded that the KMH experiment appears to be calibrated except for the largest waves, i.e., there appears to be no systematic bias of the modeled data set conditioned upon the expectation of the observed data. There is a slight tendency of the radar to show too high waves, in particular, for buoy wave heights more than about 1 m.

From a statistical perspective, buoy, radar, and KMH data may be regarded as realizations of random processes. In the following, we test the null hypothesis whether all three samples (buoy, radar, and model) can be considered as realizations of the same random process, i.e., whether they stem from the same population or whether systematic differences suggest the rejection of this hypothesis. For us to do so, the data were subsampled such that only time steps for which buoy, radar, and model data have been available are taken into account. The resulting sequence was ordered in time but had no fixed time step. Instantaneous differences between buoy and radar data have been computed. The standard deviation (σ) and the lag-1 autocorrelation (α) of these differences have then been used to model the differences by a first order autoregressive process [AR (1)-process] (von Storch and Zwiers 1999):

$$x_t = \alpha x_{t-1} + z_t \tag{1}$$

Here, x_t represents instantaneous differences at time t; z_t is a white noise with variance σ. Subsequently, 10,000 realizations k of this AR (1)-process have been obtained from Monte Carlo simulations and the realizations k of the wave height y_t^k at DWP have been computed from

$$y_t^k = b_t + x_t^k \tag{2}$$

where b_t represents the buoy measurements. Assuming that all three samples are realizations of the same random process it is expected that 95% of all radar and model data fell within a 95% confidence interval for each time-step. The result of this exercise is shown in Fig. 5. It can be inferred that, for most of the time, buoy, radar, and K-model indeed fall within the range given by 95% of the Monte Carlo simulations. In particular, this comprises 95% of the K-model and 96% of the radar data. The null hypothesis (model and observations are realizations of the same population) thus cannot be rejected with 5% error probability. It is finally concluded that the KMH shares some resemblance with reality and in the following will therefore be considered as a "substitute reality."

Comparison of near-shore extreme wave statistics from hindcasts with different spatial resolutions

In the previous section, we showed that differences between model and observations at DWP can partially be attributed to the driving HFG hindcast. It was also demonstrated that the null hypothesis, KMH, radar, and buoy data representing realization of the same random process could not be rejected at 95% confidence level. We assume in the following that the small-scale features simulated by the K-model share some resemblance with reality based on the previous statement. We will therefore consider the KMH experiment as a substitute for reality. This allows us to test to what extent improvements in the representation of near-shore extreme wave events can be achieved with several statistical downscaling techniques. The improvement will be assessed relative to the HFG hindcast, as these data are readily available and thus can be considered as a first guess of the prevailing near-shore wave conditions.

We first investigate the extent to which the HFG hindcast may be used to reasonably assess long-term wave statistics in the coastal zone. We focus mainly on the statistics of extreme events, as they are essential for coastal protection. Three data sets are analyzed, namely, significant wave height from the HIPOCAS coarse grid hindcast with about 50-km resolution (HCG), the HIPOCAS fine grid hindcast with about 5-km resolution (HFG) driven by the HCG simulation, and the KMH hindcast with 100-m resolution driven by the HFG run.

Figure 6 shows a comparison between the 99-percentiles of significant wave height for the period 1990–2001

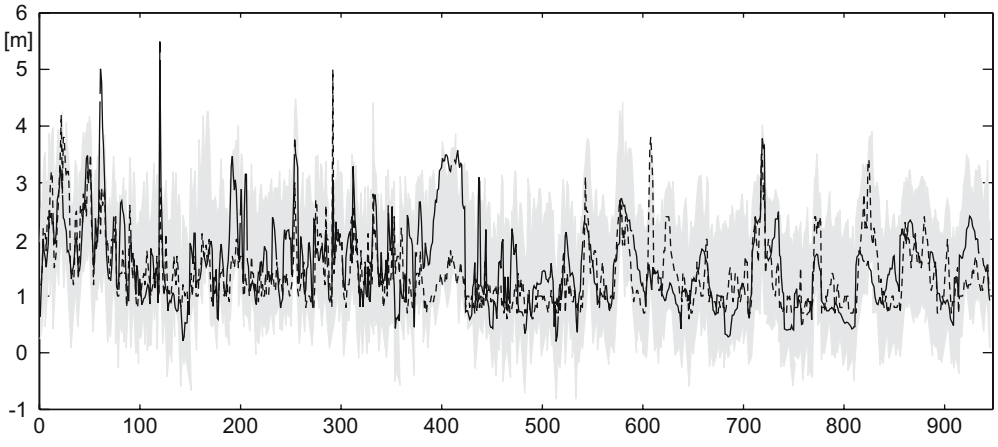

Fig. 5 Significant wave height in meters at DWP obtained from radar measurements (*dashed*) and the KMH (*solid*). The *shadowed area* shows the 95% confidence interval obtained from the Monte Carlo experiments. The analysis is made for the period October 1998–August 2001, with data gaps being excluded from the analysis resulting in 945 values

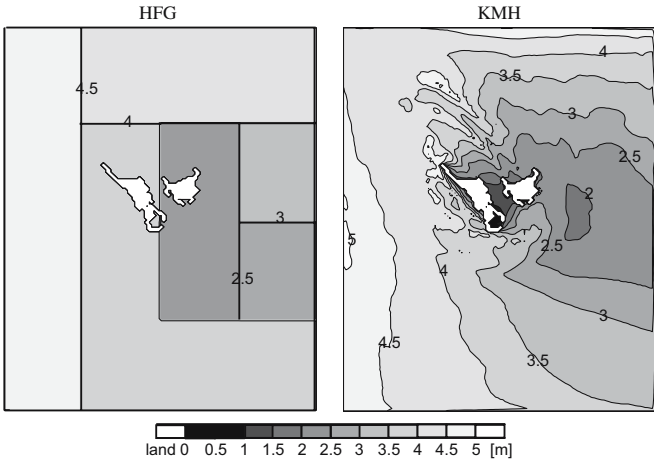

Fig. 6 Ninety-nine percentile of significant wave height in meters derived from 3-hourly values for the period 1990–2001 from the HFG hindcast (*left*) and KMH experiment (*right*)

obtained from the HFG and in the K-model hindcasts. It can be inferred that for the two simulations a similar large-scale pattern of extreme wave statistics is reproduced. The pattern is characterized by the highest waves occurring in the western part of the K-model domain that continuously decrease eastwards. A distinct area on the east of Helgoland with relatively low wave extremes can be found, which is mainly caused by the shadowing effect of the islands against the prevailing wind and wave directions. The large-scale similarity between the two simulations is primarily a consequence of the two simulations having identical wave conditions at the K-model boundaries, or in other words, that the K-model uses boundary conditions from the HFG hindcast. In addition, the same wind fields have been used in the two simulations.

Despite the large-scale similarity between the HFG and the KMH hindcasts small-scale differences in extreme wave statistics are obvious (Fig. 6). The island shadow effects are particularly more pronounced and extend further eastward in the K-model simulation. Southeastwards of Helgoland, the 99-percentile of significant wave height is about 1 m higher compared to the HFG simulation. Furthermore, for the K-model run, small-scale features of the bathymetry are visible in the distribution of the wave extremes.

While large-scale features of extreme wave statistics are quite similar in the two simulations, the small-scale differences may be significant for coastal protection. Figure 7 shows a comparison of the frequency distribution for total significant wave height near different coastal facilities obtained from the HFG and the KMH hindcasts. The location of analysis points can be inferred from Fig. 1. Although the K-model is driven with boundary conditions from the HFG run and the two simulations utilize the same wind forcing, differences in the frequency distributions particularly for near-coastal locations do emerge. The details of these differences depend on the location. At DWP, the two hindcasts are rather similar. Here, water depth is about 22 m and the shadowing effect of the island plays a minor role as the prevailing wind and wave directions are from the southwest to the northwest. At LNA, the situation is different. LNA is also located at the western side of the island, but here bathymetry effects become important. While the lower 75% of the simulated wave height distributions are still rather similar in the HFG and the KMH, the uppermost 20% are remarkably higher in the K-model

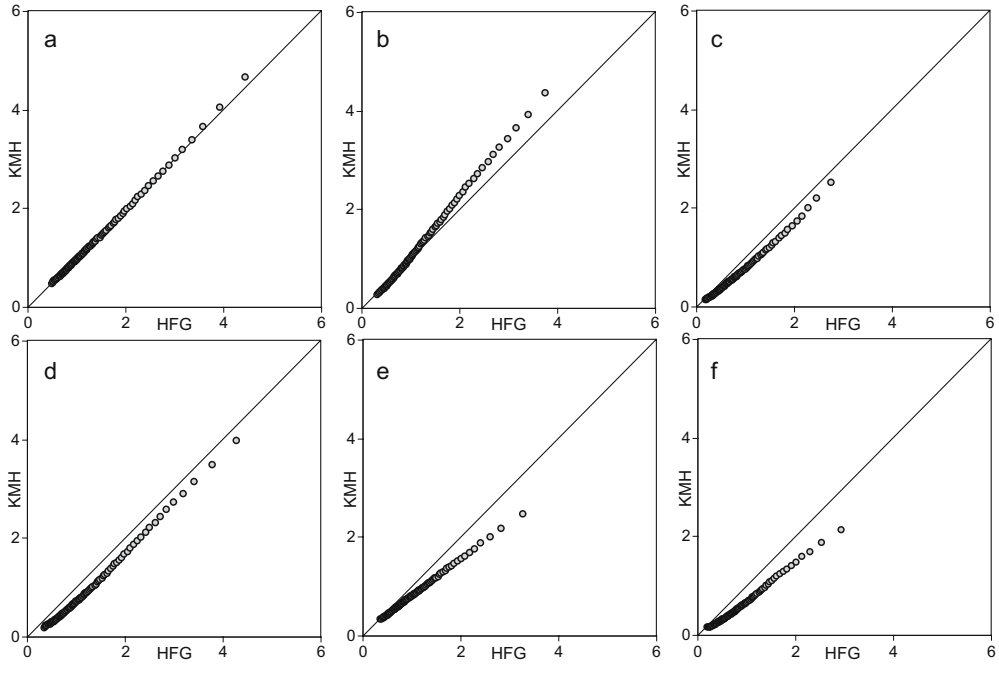

Fig. 7 Quantile–quantile plots of HFG and KMH simulated significant wave height in meters for the period 1990–2001 at points **a** DWP, **b** LNA, **c** HH1, **d** HH2, **e** DE1, and **f** DE2

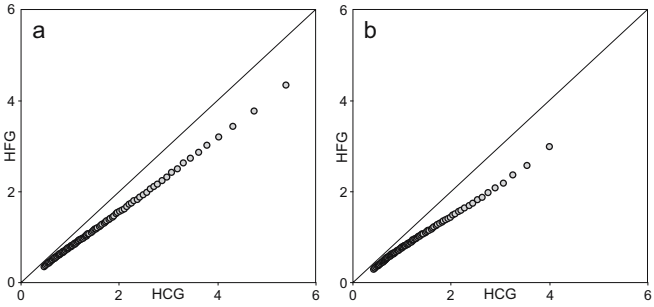

Fig. 8 Quantile–quantile plots of HCG and HFG simulated significant wave height in meters for the period 1990–2001 at points **a** LNA and **b** DE1

simulation (Fig. 7b). Near Helgoland harbor (HH1, HH2) shallow water effects and the strong gradients in the bathymetry play a significant role. Here, water depth generally reduces wave heights and waves, independent of their heights, are generally lower in KMH. East of the main island, waves are also generally smaller in the K-model hindcast. This can be inferred from the comparison of the wave height frequency distributions at DE1 and DE2, two locations near the coastal protection structures at the north and south shores of the smaller Düne Island (Figs. 7e,f). The effect is generally larger for higher waves and results mainly from a combination of lee and shallow water effects.

An analogous comparison has also been made for completeness between the HCG and the HFG hindcast. Results for LNA and DE2 are shown in Fig. 8. The situation is similar to the comparison of the HFG and the K-model hindcasts. The two simulations (HFG and HCG) utilize the same wind forcing and the coarse grid simulation provides the wave boundary conditions for the fine grid hindcast. In comparing the HCG and the HFG simulations, the same structure of results is generally obtained as in the case of the K-model and HFG hindcasts. However, while differences in the bathymetry between the HCG and HFG hindcast certainly play a role, a large fraction of the differences in the simulated wave height distribution may be attributed to the presence of the islands. While they are present in the HFG simulation, they have been neglected in the HCG hindcast, as they are too small at this resolution. As a result, waves are generally higher in the HCG hindcast.

In summary, we found that spatial resolution and shallow water effects may have a significant impact on the wave frequency distributions obtained from long-term wave hindcasts. Depending on the location, these effects can be crucial for the assessment of near-coastal wave climate, which in turn is essential for planning and construction of coastal defense. As very high resolution hindcasts (such as the one provided by our K-model simulation) are usually available only for selected cases or for restricted time periods due to their extremely high computing costs, some methodology is needed to transfer (downscale) the information that can be obtained from a multidecadal, but less well-resolved hindcasts (such as the HFG simulation), to near-shore conditions. In the following, we investigate the capability of different statistical downscaling techniques in combination with time-limited high resolution wave hindcasts (here KMH) to provide improved representation of near-shore extreme wave statistics.

Skill of different downscaling techniques in the representation of near-shore extreme wave statistics

Methods

Three different statistical approaches have been considered to test the extent to which statistical downscaling in combination with high-resolution dynamical wave modeling can be used to assess the near-shore wave climate. These are canonical correlation analysis (CCA), linear regression, and analogs (e.g., von Storch and Zwiers 1999). The large-scale wave field obtained from the HFG hindcast in all approaches is linked statistically to the local wave data from the K-model simulation. In the case of reliable and sufficiently homogeneous long-term measurements being available at the site of the construction, these may be used instead of the K-model data. However, when such data are not available or if information is required also for some surrounding area, a very high-resolution wave model simulation (such as KMH) validated with at least some existing data will represent the best possible option.

Usually downscaling techniques such as CCA or analogs are applied to monthly, annual or seasonal statistics (e.g., Zorita and von Storch 1999). However, some applications, such as the simulation of ship movements, would require high-resolution instantaneous data. We therefore extended the downscaling concept and tested here its skill in the estimation of 3-hourly wave data. Instead of directly linking large and small-scale wave statistics, all statistical models relate 3-hourly wave data from the HFG and the K-model hindcast, and statistics have been computed subsequently for comparison. For simplicity and as a first step in the following, all analyses are limited to significant wave height (SWH) only.

The K-model hindcast period was split into a 5-year fitting period (1990–1994) and a 7-year validation period (1995–2001) to fit and test the statistical models. For linear regression (LR), 3-hourly SWH and wind direction from a single grid point in the HFG simulation located near the southwestern boundary of the K-model domain have been chosen as predictors. The regression model is conditioned upon the wind directions such that eight different regression models are built depending on wind coming from the 45-degree eight sectors starting from [−22.5, 22.5]. For each grid point i in the K-model domain and each of the eight-wind direction sectors j, a regression model

$$y_{i,t} = a_{i,j}x_t + b_{i,j} \tag{3}$$

was built, where $y_{i,t}$ represents downscaled wave height, and x_t represents the predictor (HFG wave height) . The

coefficients $a_{i,j}$ and $b_{i,j}$ were fitted using a least-square method.

For the CCA, empirical orthogonal functions (EOFs) (e.g., von Storch and Zwiers 1999) have been computed for the HFG and the K-model SWH anomaly fields. For the HFG hindcast, the leading two EOFs explain about 99.1% and for the K-model hindcast about 98.3% of the total SWH variability. CCA patterns were computed subsequently based on the two leading EOFs, and SWHs for the validation period have been derived on the basis of those patterns.

For the analog method, a pool of analogs was constructed from the 3-hourly SWH fields 1990–1994 of the K-model hindcast and the corresponding principal components of the two leading EOFs of the 3-hourly HFG SWH anomaly field were computed. An analog for each date of the validation period was then determined. For this, the HFG SWH data of the validation period were projected onto the first two EOFs for the fitting period and for each pair of obtained principal components the nearest pair (analog) from the fitting period was determined. The K-model wave height field that belongs to this pair was then selected as analog wave height field for the corresponding date in the validation period.

Results

Results from the different techniques have been compared with that from the KMH simulation to test the skill of the different downscaling methods in representing near-shore wave climate and statistics. Table 1 shows the bias and the standard deviation of the error at the various locations for the different downscaling models. It can be inferred that the error is largest generally when coarse grid data from the HFG simulation are used directly to estimate the wave conditions at the near-shore locations. For linear regression and CCA, the results are comparable with LR providing slightly smaller error with standard deviation up to 0.17 m and bias less that 0.02 m depending on the location. Errors for the analog method are generally larger and sometimes comparable to that of the HFG simulation.

Figure 9 shows a comparison of wave frequency distributions obtained from the different statistical models and the HFG with KMH simulation. It can be inferred, despite the differences in representing instantaneous values, that the capability of the statistical models in reproducing the wave statistics of KMH run appears reasonable. The degree of agreement slightly differs depending on location. The quantile–quantile plot of the KMH with the HFG reference run is also shown for comparison. For deepwater points (DWP), the agreement between downscaled and KMH-derived frequency distributions is comparable for linear regression, CCA, and HFG. For the areas where the influence of topography (LNA) and other external forces (e.g., DE1, DE2) is larger, the distributions obtained from downscaled data are closer to that derived from the K-model for all the methods, while that derived from HFG provides stronger systematic deviations.

We compared the 99% of SWH at each grid point for the validation period 1995–2001 to assess the skill of different downscaling techniques in representing extreme wave statistics in the entire model domain. The skill was measured using the Brier skill score (B) (von Storch and Zwiers 1999).

$$B = 1 - S_{for}^2 \Big/ S_{ref}^2 \tag{4}$$

Here S_{for}^2 and S_{ref}^2 represent the mean squared errors of the "forecast" (in our case provided by different downscaled data sets LR, CCA and analog) and "reference forecast" (here HFG hindcast) with respect to observational data. The K-model simulation represents our substitute reality in place of missing observations. Thus, any positive value of B indicates that the downscaling method represents an improvement relative to the HFG data. The best performance corresponds with B equal to 1, which means that downscaled data are as good as "observations." A negative value of B indicates that the method performs worse than the HFG reference. The result is shown in Table 2. It is evident that all statistical methods introduce enormous additional skill in representation of the spatial distribution of the SWH 99-percentile relative to using data from the

Table 1 Bias and standard deviation of errors in meters between significant wave heights obtained from KMH and different downscaling techniques for the points near coastal facilities

STDEV(error) (m)	DWP	LNA	HH1	HH2	DE1	DE2
KMH–HFG	0.159	0.302	0.191	0.286	0.272	0.289
KMH–LR	0.097	0.163	0.104	0.159	0.128	0.085
KMH–CCA	0.108	0.255	0.179	0.19	0.163	0.13
KMH–Analog	0.224	0.364	0.234	0.385	0.218	0.184
BIAS (m)						
KMH–HFG	−0.04	0.045	−0.17	−0.257	−0.228	−0.39
KMH–LR	−0.004	−0.011	0.0002	−0.0008	−0.019	0.0006
KMH–CCA	−0.005	−0.023	0.015	−0.004	−0.025	0.009
KMH–Analog	−0.012	−0.022	0.007	−0.012	−0.2	0.004

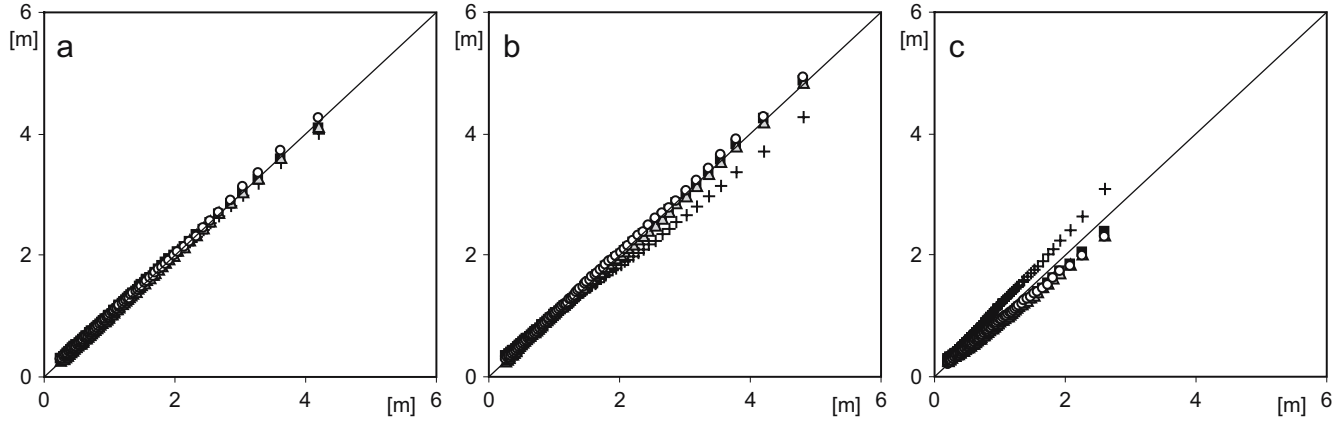

Fig. 9 Quantile–quantile plots of simulated significant wave height with different techniques in meters for the period 1990–2001 at points **a** DWP, **b** LNA, and **c** DE1. HFG (*crosses*), LR (*black squares*), CCA (*triangles*) and Analog (*circles*) at *y-axis* against KMH (*x-axis*)

HFG hindcast directly. The skill varies depending on the method from 0.975 to 0.992. This means that the improvement is in the same order of magnitude independent of the chosen statistical technique. It is therefore suggested that in the face of limited computer resources and compared to the direct use of less well-resolved data, high-resolution wave model simulations, in combination with coarse grid boundaries and statistical downscaling approaches, can yield an improved representation of extreme wave statistics for near-coastal areas.

Summary and discussion

Different approaches for obtaining high-resolution nearshore wave statistics have been considered. A high-resolution wave simulation (KMH), based on an existing multidecadal wave hindcast for the North Sea, for the area around Helgoland for the period 1990–2001 was performed and found to reasonably represent observed wave conditions. Results of the KMH simulation were compared with the buoy and radar wave observations. The results demonstrated that the simulated wave data (SWH, peak period, and peak direction) generally show good agreement with measurements in terms of distributions, although upper percentiles of the modeled SWH appeared to be overestimated. The latter is partially caused by the boundary conditions that provide too high waves in case of severe storms. As differences occur also between different measurements (buoy, radar), we tested whether the range of errors between observed and modeled data is comparable to that between different measurements and whether model and observations can be considered as realizations of the same random process. It was found that this hypothesis could not be rejected with 5% error probability, indicating that there is some skill in the KMH wave simulation.

As an alternative to time-consuming high resolution wave modeling, the use of less expensive statistical–dynamical methods to obtain detailed wave statistics was investigated. Three statistical methods, namely linear regression, CCA, and analogs were examined. It was found that all three methods considerably improved the estimation of extreme wave statistics compared to the driving large-scale hindcast and can be used as alternatives in case of limited computing resources.

The methods, so far, have been applied only to SWH, and most of the study is founded on SWH statistics. Although SWH represents one of the most frequently analyzed and most crucial wave parameter, other parameters are important for particular applications. For instance, from wave periods and wave heights, wave steepness can be inferred, which represents an important criterion in the design of ships and vessels. Another example that depends on wave period is the derivation of wave-induced bottom stress, which is important for the sediment transport and coastal erosion evaluations. Other parameters, such as wave direction, are crucial especially for extreme wave analysis within the coastal protection problem where it is important to know from which direction the severe waves are coming. Nevertheless, we concentrate here on SWH as a starting point and propose to extend the methodology to other wave parameters in future studies.

Turning to the discussion of the potential limitations and benefits of the downscaling methods, we start from the analog. As it can be inferred from Tables 1 and 2, this method shows the worst performance among the tested methods in terms of error deviation. At the same time, the data obtained with the analog method are not more biased than that from other statistical methods. This unbiased but too variable behavior can be partially explained by incompleteness of the analog pool, i.e., for this method, a fitting period longer than 5 years is required to accumulate the

Table 2 Brier scores for the 99-percentile of SWH from 3 statistical methods

LR	CCA	Analog
0.992	0.98	0.975

sufficient set of significant wave height patterns. This problem could be a strong limitation in case of applications to scenario studies, as wave situations that did not occur during the fitting period or were not included in the analog pool cannot be detected and reproduced by this method. The results of the CCA are quite close to that from the KMH simulation, but the computational costs for CCA are higher than that for LR and analogs. The linear regression model shows the best results in comparison with the dynamically downscaled data (Tables 1 and 2) and gives the opportunity for the construction of more than one integrated wave parameter.

Based on a balance between the quality of simulated data and required computational resources, LR appeared to be the most acceptable method for downscaling long-term wave data and obtaining small-scale wave statistics. It solves the problem of insufficient time and space resolution presented in multidecadal wave hindcasts and extremely high computational costs for long-term high resolution wave hindcasts. We conclude that the combination of existing coarse grid long-term wave hindcasts (such as HFG) with shallow water wave modeling for short time periods and linear regression represents a cost-efficient way to estimate near-shore wave climate and to provide required statistics for coastal management needs.

Acknowledgements We would like to thank Gerhard Gayer and Heinz Günther for the numerous valuable discussions and help with the K-model. We are grateful to Dieter Schrader from the BSH (Federal Maritime and Hydrographic Agency) and Olaf Outzen from Oceanwaves GmbH for providing us with observational data and useful comments. We want to thank Eduardo Zorita who helped us with statistical methods, provided subroutines for the Analog and CCA methods and gave useful advice. We also thank Norbert Winkel and Andreas Pluess from BAW for kindly providing topography and water level data.

References

Caires S, Sterl A, Bidlot J-R, Graham N, Swail V (2002) Climatological assessment of reanalysis ocean data. In: Proceedings of the 7th international workshop on wave hindcasting and forecasting, Banff, Alberta, Canada, 21–25 October 2002

Cavaleri L, Rizzoli PM (1981) Wind wave prediction in shallow water — theory and application. J Geophys Res 86:10961–10973

Coastal Engineering Manual, CHL, available at http://chl.erdc.usace.army.mil

Cox AT, Swail VR (2001) A global wave hindcast over the period 1958–1997: validation and climate assessment. J Geophys Res 106(C2):2313–2329

Eurowaves project, available at http://www.oceanor.no/projects/eurowaves

Feser F, Weisse R, von Storch H (2001) Multi-decadal atmospheric modeling for Europe yields multipurpose data. EOS Trans 82 (28):305–310

Günther H and Rosenthal W (1995) A wave model with nonlinear dissipation source function. In: Proceedings of the 4th International workshop on wave hindcasting and forecasting, Banff, Canada, 16–20 October 1995

Günther H, Rosenthal W, Stawarz M, Carretero JC, Gomez M, Lozano I, Serrano O, Reistad M (1998) The wave climate of the Northeast Atlantic over the period 1955–1994: the WASA wave hindcast. Global Atmos Ocean Syst 6:121–163

Hasselmann K (1974) On the spectral dissipation of ocean waves due to white capping. Boundary–Layer Meteorol 6:107–127

Hasselmann K, Barnett TP, Bouws E, Carlson H, Cartwright DE, Enke K, Ewing JA, Gienapp H, Hasselmann DE, Kruseman P, Meerburg A, Müeller P, Olbers DJ, Richter K, Sell W, Walden H (1973) Measurements of wind–wave growth and swell decay during the Joint North Sea Wave Project (JONSWAP). D Hydrogr Z A8(12):1–95

Hessner K, Reichert K, Dittmer J, Nieto Borge JC, Günther H (2001) Evaluation of WaMoS wave data. In: Proceedings of the WAVES 2001 conference, San Francisco, 2–6 September 2001

JERICHO project, available at http://www.satobsys.co.uk/Jericho

Kushnir Y (1997) The recent increase in North Atlantic Wave Heights. J Climate 10(8):2107–2113

Moghimi S, Gayer G, Günther H, Shafieefar M (2005) Application of 3rd generation shallow water wave models in a tidal environment. Ocean Dyn 55(1):10–27

Schneggenburger C (1998) Spectral wave modelling with nonlinear dissipation. Ph.D. thesis, University of Hamburg

Schneggenburger C, Günther H, Rosenthal W (1997) Shallow water wave modelling with nonlinear dissipation, Dtsch Hydrogr Z 49:431–444

Soares CG, Weisse R, Carretero JC, Alvarez E (2002) A 40-years hindcast of wind, sea level and waves in European waters. In: Proceedings of the 21st international conference on offshore mechanics and arctic engineering, Oslo, Norway, 23–28 June 2002

Sterl A, Komen GJ, Cotton PD (1998) Fifteen years of global wave hindcasts using winds from the European Centre for medium-range weather forecasts reanalysis: validating the reanalyzed winds and assessing wave climate. J Geophys Res 103:5477–5492

Vierfuss U (2002) Ermittlung der Seegangsbelastung für Helgoländer Molenbauwerke. Hansa 139:68–73

von Storch H, Zwiers FW (1999) Statistical analysis in climate research. Cambridge University Press, Cambridge

WAMDI Group (1988) The WAM model — a third generation ocean wave prediction model. J Phys Oceanogr 18:1775–1810

WASA Group (1998) Changing waves and storms in the Northeast Atlantic? Bull Am Meteorol Soc 79(5):741–760

Weisse R, Feser F, Günther H (2002) A 40-year high-resolution wind and wave hindcast for the Southern North Sea. In: Proceedings of the 7th international workshop on wave hindcasting and forecasting, Banff, Alberta, Canada, 21–25 October 2002, pp 97–104

Weisse R, Feser F, Günther H (2003) Wind-und Seegangsklimatologie 1958–2001 für die südliche Nordsee basierend auf Modellrechnungen. GKSS 2003/10 GKSS Forschungszentrum

Zorita E, von Storch H (1999) The analog method as a simple statistical downscaling technique: comparison with more complicated methods. J Climate 12:2474–2489